

# Heat Transfer and Phase Transformation on Matrix Assisted Pulsed Laser Evaporation (MAPLE) of Biocompatible Thin Layers

E. Lacatus<sup>1\*</sup>, M.A. Sopronyi<sup>2</sup>, G.C. Alecu<sup>3</sup>, A. Tudor<sup>3</sup>

<sup>1</sup> UPB – Polytechnic University of Bucharest; <sup>2</sup>INFLPR – National Institute for Laser Plasma and Radiation Physics; <sup>3</sup>UPB – Polytechnic University of Bucharest – Student

\*E. Lacatus, Assoc. Prof.: UPB- IMST, 313 Splaiul Independentei , RO-060032, email: [elena.lacatus@upb.ro](mailto:elena.lacatus@upb.ro)

**Abstract:** Matrix Assisted Pulsed Laser Evaporation (MAPLE) technique is used for the deposition of high quality biocompatible polymer thin films, such as polyvinylpyrrolidone (PVP), from 2% PVP in dimethyl sulfoxide (DMSO) solution. During the entire deposition process the temperature of the laser target should be kept below 193K to assure the proper quality of both evaporation and deposition phases of the process. On a first approach COMSOL Multiphysics was used to describe and analyze the current cooling technology using liquid He<sub>2</sub> and N<sub>2</sub>. The SolidWorks model of the present MAPLE technique was exported through Livelink in COMSOL in order to identify the present bottlenecks of the process. Addressing the identified issues of the process, a new cooling technology (Pulse Tube Refrigeration – PTR) was designed to assist the MAPLE technique. COMSOL Multiphysics enabled the simulation of the temperature flux distribution during both MAPLE techniques, making possible the accurate interface phenomena analysis.

**Keywords:** nanostructure, biocompatible, MAPLE, heat transfer, FEA

## 1. Introduction

Biocompatible nanostructured thin films can be obtained through several methods: dip coating [1], Langmuir Blodgett [2], layer-by-layer [3], Pulsed Laser Deposition (PLD) [5], etc. During the PLD process a bulk material target is irradiated by a laser beam. Under the heating process, and phases changes, the bulk material is reaching the plasma state in the space between the surface of the laser target and the surface of the substrates holder; afterward, cooling layer-by-layer on the substrate. A more accurate method to obtain biocompatible nanostructured thin layers from organic frozen compounds is MAPLE [4] (Fig.1). This is a laser technique rooted from PLD, but in this case a frozen

solvent matrix is used to protect the biocompatible compound from the thermal effect of the laser pulses. However, the solvent and the organic compound are mixed and frozen before the MAPLE technique application, and the laser beams energy is much lower than that used in PLD method [6-8].

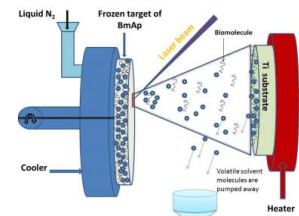


**Figure 1** MAPLE technique

Thus, on MAPLE there is no more plasma during the deposition process, but an evaporation followed by a condensation on the substrate. As soon as the evaporated mixture reaches the pre-heated surface of the substrate (320K), the solvent is evaporated, and an organic film of  $\sim 100\text{\AA}/\text{pulse}$ , on up to 20.000 pulses of 25ns each, at a frequency of 10 Hz high, is condensed layer-by-layer on the substrate.

On this study the SolidWorks model of the MAPLE reaction chamber, having attached a cooling system with an adjacent cooling agent (N<sub>2</sub> liquid) holder (Fig. 2 a,b), was exported through Livelink to COMSOL Multiphysics.

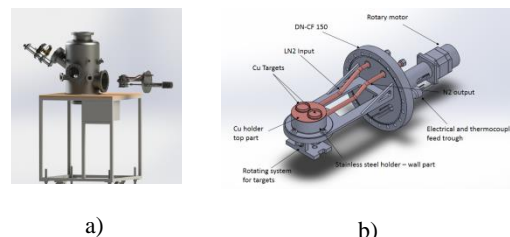


**Figure 2** Classic cooling system. a) MAPLE chamber, b) MAPLE assembly

A simulation of the temperature distribution of DMSO, inside the rotating Copper target, has been done using FEA in COMSOL (Fig. 3). The

thermal distribution analysis within the DMSO sample cooled by the adjacent holder (liquid N<sub>2</sub> at 77K) illustrates that during MAPLE deposition under 25ns laser pulses, the DMSO target changes its phase state from solid to liquid, and from that on the thin layer deposition cannot occur any more.

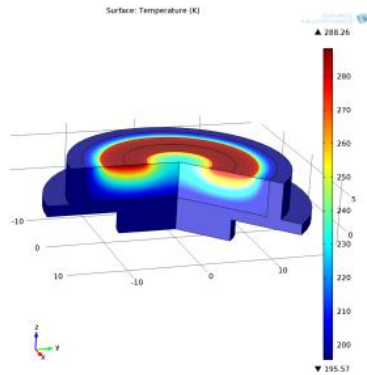


**Figure 3** Temperature distribution of an target (DMSO+2%PVP) in an classic cooling system

After this analysis a new heat transfer system was designed to assist the MAPLE technique aiming to maintain the adequate values of the parameters across both evaporation and deposition phases of the process. The Pulse Tube Refrigeration cooling system has been designed to fit the technical data of the MAPLE reaction chamber (Fig.4). Its SolidWorks model was as well exported through Livelink in COMSOL Multiphysics and a new thermal distribution on the DMSO sample was determined (Fig. 5) for the Copper target rotating all together with the PTR system.



**Figure 4** Chamber assembly for MAPLE with PTR cooling

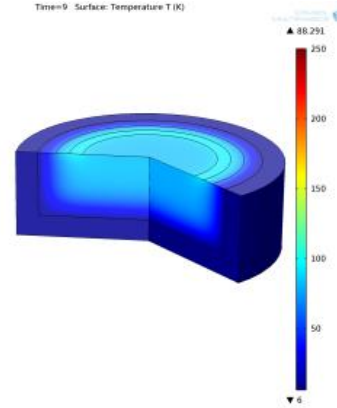


**Figure 5** Temperature distribution of an target (DMSO+2%PVP) in PTR cooling sys

## 2. Governing Equations

For the Copper target cooled through an adjacent holder the thermal distribution within the laser target is governed by the Equation 1 [9]:

$$\rho(T) \cdot C_p(T) \frac{\delta T(x,z,t)}{\delta t} = \nabla \cdot [k(T) \cdot \nabla T(x,z,t)] + Q(z,t) \quad (1)$$

where:  $x$  and  $z$  are space coordinates ( $z$  being the normal to the surface);  $\rho$  is the mass density;  $C_p$  the specific heat at constant pressure;  $k$  is the thermal conductivity of the material.  $Q(z,t)$  is the amount of energy absorbed within the target during a laser beam pulse, being expressed by the Equation 2 [9]:

$$Q(z,t) = I_S(z,t) \times (1 - R) \times A_C \exp(-A_C z) \quad (2)$$

where:  $I_S(t)$  is the temporal irradiance on the surface of the target;  $R$  is the reflectivity of the material, and  $A_C$  is the absorbance of the target. The temporal laser irradiance is governed by the Equation 3 [9]:

$$I_S(z,t) = I_0(z,t) \exp\left(\frac{-3.5(t-\tau_m)}{\tau^2}\right) \exp\left(-\frac{x^2}{r^2}\right) \quad (3)$$

where:  $I_0$  is the intensity of the laser on target (W/cm<sup>2</sup>), and the second part of the equation represent the Gaussian profile of the laser, where  $\tau_m$  is the time at which the power is maximum ( $\tau_m = 25$ ns for full width at half maximum - FWHM, and a maximum pulse energy of 700mJ),  $x$  is the position of the laser,  $r$  is the radius of the laser beam

The absorption coefficient of the target  $A_c$  was determined with Equation 4 [10]:

$$A_c = \frac{1}{\delta_a} = \frac{2\omega n_2}{c} = \frac{2\pi n_2}{\lambda} \quad (4)$$

where:  $\delta_a$  represents the penetration length,  $\omega$  is the circular frequency,  $n_2$  is the extinction coefficient,  $c$  is the speed of light in vacuum and  $\lambda$  is the wave length of the laser beam. From experimental data it was determined that the penetration length is  $\delta_a \approx 9\text{nm}$ .

For the calculation of  $n_2$ , one has to use the Equation 5 [10]:

$$n_c = n_1 + in_2 \quad (5)$$

where:  $n_c$  is the complex reflective index, and  $n_1$  is the refractive index of the material.

The main difference between the use of an adjacent cooling system and a PTR sys is given by the Equation 6 [COMSOL tutorial]:

$$q_{target}(r, T, t) = \frac{\mu \times F_n}{A_s} \omega_t \times r + \Delta T \quad (6)$$

where:  $\mu$  is the coefficient of dry friction;  $F_n$  – the normal force on the target;  $A_s$  – contact surface between the target and cooling agent holder;  $\omega_t$  is the angular velocity of the target (rad/s) and  $r$  is the radius of the target.

### 3. Methods

The FEA of the Copper target containing 5mL of (DMSO+2%PVP) under the effect of laser beam pulses produced by COMPLEX Pro 205 KrF excimer laser has been done for a laser beam having the following characteristics: wave length  $\lambda=248\text{nm}$ , pulse  $\tau_m = 25\text{ns}$  for full width at half maximum (FWHM) and maximum pulse energy  $Q_m = 700\text{mJ}$ . Previous studies have revealed that for this specific deposition a fluence (Energy/surface [ $\text{J}/\text{cm}^2$ ]) of  $4 \text{ J}/\text{cm}^2$  is required.

During the MAPLE process the Copper target is rotating with 60RPM. In the case of the use of an adjacent cooler the rotation between this cooler and the MAPLE reaction chamber is taking place with friction; in the case of PTR sys (Fig.6) the entire assembly (Copper target and PTR sys) is rotating all at once. The PTR sys is a

cryocooler without moving parts, needing no liquid bath cryostat within its structure. Actually, the Pulse Tube is a simple tube having one open end and one closed end. The closed end is the hot end is being capped with a heat exchanger cooling it to the ambient temperature. The open end is the cold end, being connected with the regenerator and a cold stage of a second heat exchanger. The regenerator is a periodic flow heat exchanger [13]

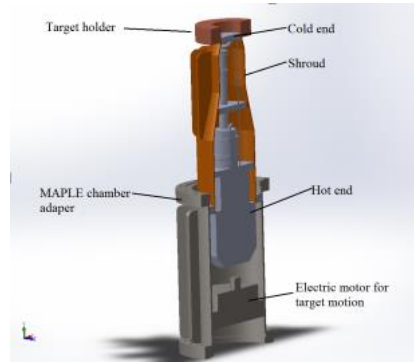


Figure 6 Section view in PTR assembly

### 4. Theory

The use of Pulse Tube Refrigeration is supposed to eliminate the impediments of heating during friction of the relative moving of the parts of the system. As well PTR is working on a greater temperature range offering a better control of the nominal temperature. Coupling it with control software and adequate sensors harvesting real time data from the process, users may choose almost any nominal temperature from a wide range [13].

### 5. Numerical Model

The model of the system was designed with the use of a 2D-axisymmetric representation, thus the coordinates used in the equations have been changed to:  $r$  for  $x$ , and  $z$  for  $y$ . The parameters used for the finite element simulation are on Table 1. From equation 2,  $Q(z, t)$  was written using the *variables* section of COMSOL, under *model 1* for the DMSO domain, as [11]:

$$Q_{target} = I \cdot (1 - R_c) \cdot A_c \cdot \exp(-A_c(z)) \cdot \sin^2(\omega t) \quad (7)$$

where:  $I$  is the intensity of the laser on the target surface multiplied with the Gaussian of the laser in time and space[14], as (Fig.8) :

$$I=I_0 \cdot \text{Gauss\_time}(t) \cdot \text{Gauss\_space}(r) \quad (8)$$

where:  $\text{Gauss\_time}$  and  $\text{Gauss\_space}$  (Fig.7) are analytical functions defined in the *global definitions* as (Fig.4):

$$\text{Gauss\_time} = \exp(-3.5((t-\tau_m)/(t-\tau_m))/(\tau_m \cdot \tau_m)) \quad (9)$$

$$\text{Gauss\_space} = \exp(-(r^2/r_0^2)) \quad (10)$$

with the arguments  $t$ , and arguments for unit  $s$ ; and in the plot parameters, for  $t$  -  $[0, 10e-8]$ , and argument  $r$ , and argument for unit  $mm$ , and in the plot parameters:  $r$ - $[-10e-5, 10e-5]$ . In order to simulate a pulsed laser beam, in the heat Equation 7, the heat flux distribution was multiplied with  $an2(t)$  (Fig.8).

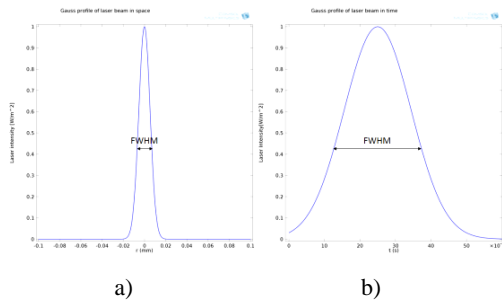


**Figure 7** Gaussian profile of the laser beam depending of a) space and b) time

The function  $an2(t)$  has the expression of a triangle function  $tri1(t)$ , with the arguments  $t$ , unit arguments  $s$ , and plot parameters  $t$  -  $[0, 10 \cdot \tau_m]$ , and periodic extension of  $[0, 2 \cdot \tau_m]$ . The triangle function  $tri1(t)$  mentioned earlier has the lower limit  $\tau_m/2$  and the upper limit  $\tau_m/2 + \tau_m$ .

For the friction section, equation (6) was written as [12]:

$$Q_{\text{contact}} = (\mu \cdot F_n / A_{\text{contact}}) \cdot (R \cdot \omega) + \text{step1}((T_{LN2}) [1/K]) \quad (11)$$

Where  $R$  has the expression:

$$R = \sqrt{2 \cdot r^2} \quad (12)$$

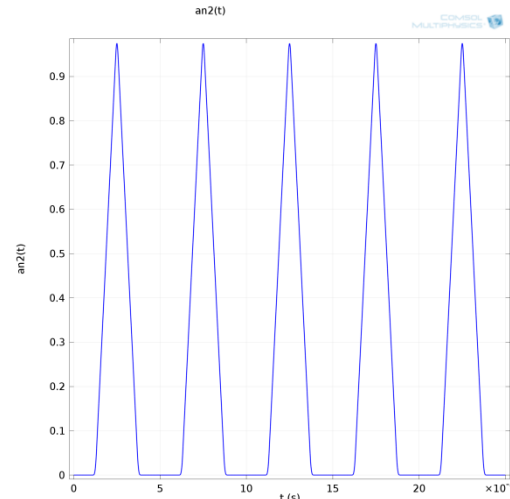


**Figure 8** Graph of an pulsed laser deposition at 10[Hz]

The term  $step1(T_{LN2})$  from Equation 11 denotes the transition from the temperature of 293.15 K to 77 K, where the function  $step1$  is  $293.15 \div 77$  with a smoothing of 0.1.

Equation 11 it is written in the variables section, with a condition applied to the boundary that is in contact with the cooling agent holder.

The copper target model was analyzed using the COMSOL modules *Heat transfer in Solids* with the features *Heat Source* with equation (7) and *Heat Flux*, that where applied to the mesh, with equation (13).

$$q_0 = h \times (T_{ext} - T) \quad (13)$$

where:  $q_0$  is the heat flux ( $W/cm^2$ ),  $h$  - heat transfer coefficient,  $T_{ext}$  external temperature;  $T$  - object temperature.

Using the mesh structure of the target model, time depending studies were computed for both models (cooler and PTR) and the results have been processed.

## 6. Experimental Results

As an output of the numeric model analyses, the following graphics have been obtained:

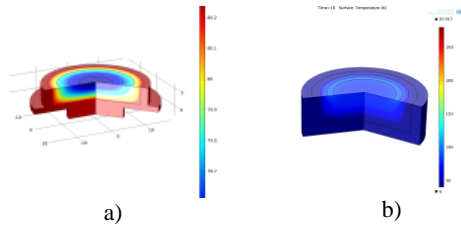


**Figure 9** Thermal distribution due to friction in *a)* LN2 cooling agent and *b)* PTR cooling

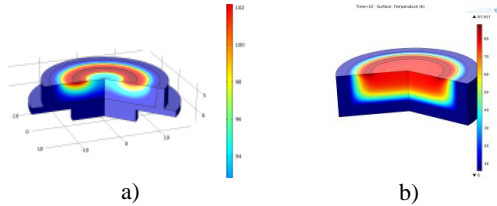


**Figure 10** Thermal distribution due to laser irradiation in *a)* LN2 cooling agent and *b)* PTR cooling

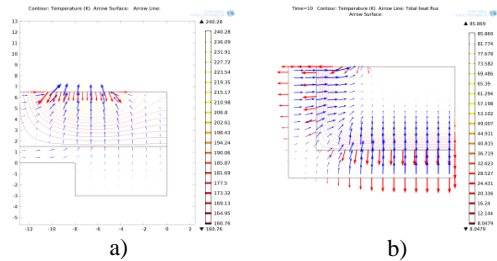


**Figure 11** Isothermal contour within the target in *a)* LN2 cooling agent and *b)* PTR cooling

**Table 1** Simulation parameters

F_n	231[N]	Target normal force
r_target	17[mm]	Radius of the target
r_down	4[mm]	Radius of the down part of the target
A_contact	$\pi \cdot (r_{\text{target}}^2 - r_{\text{down}}^2)$	Contact area
T_amb	293.15[K]	Temperature in the chamber
T_LN2	77[K]	Liquid nitrogen temperature
n	60[1/min]	Rotation of the target
Omega	$2 \cdot \pi \cdot n$ [rad]	Angular velocity of the target
mu	1[1]	Friction coefficient Cu-Cu
Lambda	248[nm]	Laser wave length
Tau_m	25[ns]	Time for FWHM
Fluence	0.4[mj/cm^2]	Fluence on the target surface
I0	$\text{Fluence} \cdot (1/\text{tau}_m)$	Intensity of the laser on the target
D_a	9[nm]	Ablation depth
Ac	1/d_a	Absorption coefficient
Rc	0.5[1]	Reflectivity of the target
Time_step	$[1\text{s}] \cdot \text{tau}_m / 10$	Time to store solution
End_time	50[s]	Last time step

## 7. Conclusions

The use of PTR is more effective: with the liquid N<sub>2</sub> cooling system the temperature of the target goes above the melting point of DMSO at low pressure (213.15K), while by the use of PTR cooling system the

temperature of the target stays well below this threshold.

## References:

- [1] Khalid, M. , Mujahid, M., Khan, A.N., Rawat, R.S., Dip Coating of Nano Hydroxyapatite on Titanium Alloy with Plasma Assisted  $\gamma$ -Alumina Buffer Layer: A Novel Coating Approach, *Journal of Materials Science and Technology*, Volume 29, Issue 6, June 2013, Pages 557-564
- [2] Burrs, L.S., Jairam, S., Vanegas, D.C., Tong, Z., Mclamore, E.S. Lignin and silicate based hydrogels for biosensor applications, *Progress in Biomedical Optics and Imaging - Proceedings of SPIE*, Volume 8719, 2013, Article number 87190H
- [3] Mohanta, V., Madras, G., Patil, S., Albumin-mediated incorporation of water-insoluble therapeutics in layer-by-layer assembled thin films and microcapsules, *Journal of Materials Chemistry B*, Volume 1, Issue 37, 7 October 2013, Pages 4819-4827
- [4] Cristescu, R. , Doraiswamy, A., Socol, G., Grigorescu, S., Axente, E., Mihaiescu, D., Moldovan, A., Narayan, R.J., Stamatiu, I., Mihaiescu, I.N., Chisholm, B.J., Chrisey, D.B., Polycaprolactone biopolymer thin films obtained by matrix assisted pulsed laser evaporation, *Applied Surface Science*, Volume 253, Issue 15, 30 May 2007, Pages 6476-6479
- [5] Minkov, I.P. Simeonov, S., Szekeres, A., Cziraki, A., Socol, G., Ristoscu, C., Mihaiescu, I.N., Study of the charge transport mechanism in pulsed laser deposited AlN:Si films , *Journal of Physics: Conference Series*, Volume 356, Issue 1, 2012, Article number 012038
- [6] Califano, V., Bloisi, F., Vicari, L., Barra, M., Cassinese, A., Fanelli, E., Buzio, R., Valbusa, U., Carella, A., Roviello, A., Substrate temperature dependence of the structure of polythiophene thin films obtained by Matrix Assisted Pulsed Laser Evaporation (MAPLE) *EPJ Applied Physics*, Volume 48, Issue 1, October 2009, Article number 10505

[7] Motoc, M.M., Axente, E., Popescu, C., Sima, L.E., Petrescu, S.M., Mihailescu, I.N., Gyorgy, E., Active protein and calcium hydroxyapatite bilayers grown by laser techniques for therapeutic applications, *Journal of Biomedical Materials Research - Part A*, Volume 101 A, Issue 9, September 2013, Pages 2706-2711

[8] Socol, G. , Preda, N., Socol, M., Sima, L., Luculescu, C.R., Sima, F., Miroiu, M., Axente, E., Visan, A., Stefan, N., Cristescu, R., Dorcioman, G., Stanculescu, A., Radulescu, L., Mihailescu, I.N., MAPLE deposition of PLGA micro-and nanoparticles embedded into polymeric coatings, *Digest Journal of Nanomaterials and Biostructures*, Volume 8, Issue 2, 2013, Pages 621-630

[9] J. H. Bechtel, Heating of solid targets with laser pulses, *Journal of Applied Physics*, vol. 46, no. 4, pp. 1585–1593, Apr. 1975.

[10] M. Darif, N. Semmar, Numerical Simulation of Si Nanosecond Laser Annealing by COMSOL Multiphysics, *Excerpt from the Proceedings of the COMSOL*, Conference 2008 Hannover

[11] <http://www.comsol.com/model/laser-heating-a-self-guided-tutorial-12317>, last view 15.08.2013

[12] Friction Stir Welding, Comsol 4.3 Heat transfer module

[13]<http://large.stanford.edu/course/2007/ph210/bert2> last view 15.08.2013

[14] Manoj Kumar Sharma, Optimization of laser induced forward transfer by finite element modeling, Royal Institute of Technology Sweden, April 2013